

Table 1. Observed Absorption and Emission Band Maxima of DASQMI in Different Solvents at Room Temperature

solvent	dielectric constant (ϵ_r)	H bond donor ability	absorption maximum λ_{abs} (nm)	fluorescence maximum λ_{ems} (nm)
MCH	02.070	0.00	373	430
EtOH	24.50	0.93	392	522
ACN	37.50	0.19	387	524
DMF	36.70	0.00	394	524
DMSO	46.70	0.00	397	528
D ₂ O	78.30	0.00	395	529
water	80.01	1.17	374	480

Dye emission intensities are also important to consider when choosing a dye for a particular imaging application, and they have particular importance in organic light-emitting diodes (OLED). So it is envisaged in this study to investigate thoroughly the solvent effect of nonpolar, polar, highly polar, polar protic, and highly polar protic solvents and their different low-temperature dependence on the steady state, and also the time-resolved emission of DASQMI at room temperature, in the pursuit of origin of high emission. Quantum chemical calculations of DASQMI to know the geometry in the ground and excited states would also be employed.

2. MATERIALS AND METHODS

The compound 2-[4-(dimethylamino)styryl]-1-methylquinolinium iodide (DASQMI) and deuterium oxide (D₂O) were procured from Aldrich Chemical Co. and was recrystallized before use. Methylcyclohexane (MCH), cyclohexane (CYC), acetonitrile (ACN), ethanol (EtOH), *N,N*-dimethylformamide (DMF), dimethyl sulfoxide (DMSO), chloroform (CHCl₃), dioxane, and 1-butanol (1-BuOH) were from Merck Specialties Pvt. Ltd. (India) and were used as such after their emission was checked in the region of interest.

The absorption spectra were taken with a Shimadzu UV–vis absorption spectrophotometer, model UV-2401PC. The fluorescence spectra were obtained with a Hitachi F-4500 fluorescence spectrophotometer. Quantum yields were measured by a secondary standard method ($\phi_f = 0.23$) with recrystallized β -naphthol in MCH; details of the process are described elsewhere.^{20,21} Emission-wavelength-dependent anisotropy spectrum was measured on the same spectrophotometer with an additional polarizer attachment. Anisotropy was calculated by use of the formula

$$\langle r \rangle = \frac{I_{VV} - GI_{VH}}{I_{VV} + 2GI_{VH}} \quad (1)$$

where G is the grating factor that has been included to correct the wavelength response to polarization of the emission optics and detector. I_{VV} and I_{VH} are the emission intensities measured parallel and perpendicular to the vertically polarized excitation, respectively, for a particular wavelength, and for each wavelength we calculate anisotropy and plot it against wavelength.

For lifetime measurement at room temperature, the sample was excited (at 440 nm, optical density ~ 0.15) with a picosecond diode (IBH Nanoled-07). The time-correlated single-photon counting (TCSPC) set up consists of Ortec 9327, TBX-04 detector, Data-Station measurement software, and DSA6 Foundation

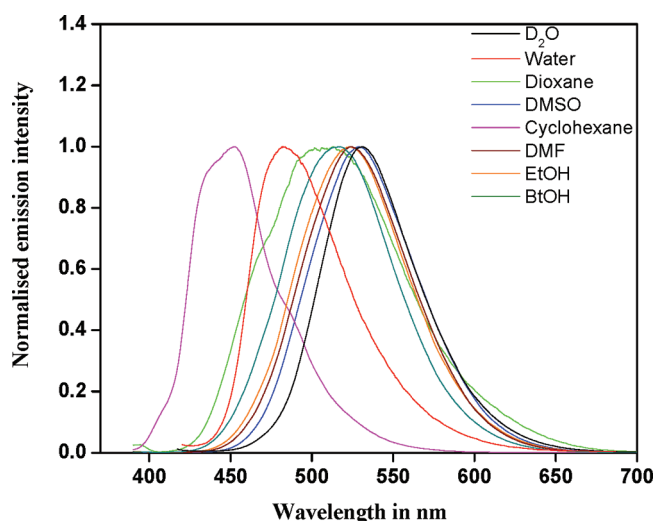


Figure 1. Emission spectra of probe molecule DASQMI in cyclohexane, dioxane, ethanol, butanol, DMF, DMSO, D₂O, and water at room temperature ($\lambda_{\text{ext}} = 390$ nm).

Package. The data were collected with a DAQ card as a multi-channel analyzer. The typical full width at half-maximum (fwhm) of the system response is about 80 ps. Typical slit width ~ 30 nm, monochromator type Jobin-Yvon, number of channels 4000 (6 ps/channel), window width ~ 24.5 ns, and number of counts $\sim 10\,000$ were used in taking decay profiles. Data analysis was carried out by use of the curve-fitting program supplied by the manufacturer. Quality of the fit was determined by reduced χ^2 and a high Durbin–Watson parameter (>1.7).²²

The ground-state (GS) geometry optimization of DASQMI in vacuum has been obtained by the unrestricted Hartree–Fock (UHF) method in Gaussian03²³ with 3-21g(+,*), and 6-31g(d,p) basis sets. The configuration interaction singles (CIS) method has been used to optimize the excited-state geometry with basis set 6-31g(d,p). Both the energy and dipole moment have been obtained from the optimized geometry in ground and excited states following the quantum chemical calculations as embedded in the Gaussian03 software package.

3. RESULTS AND DISCUSSION

3.1. Steady-State Absorption and Fluorescence Spectra. DASQMI shows absorption maxima at 373, 387, and 392 nm in MCH, acetonitrile, and ethanol, respectively, but in water the peak is at 374 nm. The red-shifted absorption spectra of the molecule were observed in solvents with higher polarity, indicating progressively greater stabilization of the excited state in a polar environment. But there is relatively greater stabilization of ground than excited state of hydrophobic DASQMI molecule in water, due to the quinonoid to benzenoid transformation, and the absorption band gets blue-shifted compared to other polar solvents like ACN and ethanol. The absorption maxima, dielectric constants, and hydrogen-bond donor abilities of the solvents are reported in Table 1. It seems that the solvent polarity may be one of the important factors for stabilizing the excited state. Figure 1 shows the fluorescence spectra of the probe molecule in different solvents. A significant shift in the peak position from 430 nm in a nonpolar solvent like MCH to 528 nm in a more polar solvent like DMSO was observed. The fluorescence

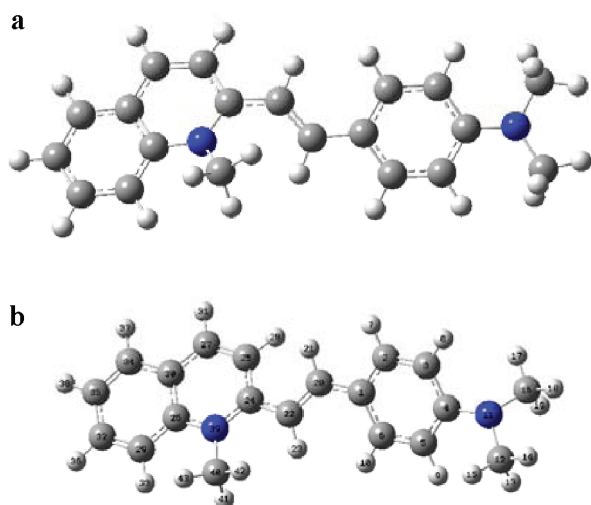


Figure 2. (a) Optimized ground-state geometry [using UHF method with 6-31g(d,p) basis set] and (b) optimized excited-state geometry [using CIS method with 3-21g(+,*) basis set].

excitation spectra of DASQMI in MCH and EtOH match well with the absorption spectra in the same solvents, which indicates that each of the emission bands arises from excitation of the same ground-state species.

In order to understand the nature of geometry of DASQMI, we performed unrestricted Hartree–Fock (UHF) calculations with basis set 6-31g(d,p) in ground state. The energy and dipole moment are $-878.527\,557\,43$ au and 0.9392 D, respectively, in gas phase. In the vertically excited Franck–Condon state (we call it “normal state” here), the energy value and the dipole moment are $-875.527\,709\,31$ au and 2.54 D, respectively, by the CIS method with basis set 6-31g(d,p) in gas phase. The optimized geometry of DASQMI in ground state (Figure 2a) is nearly planar, and in excited state (by the CIS method) the dimethylamino group is rotated nearly 90° about the single bond $N_{11}-C_4$ (Figure 2b) as well as the dimethylaminophenyl ring being rotated 180° about the single bond $C_{22}-C_{24}$ near the quinolinium ring. Tomasi’s polarizable continuum model (PCM) is also used to incorporate the solvent effect as implemented in Gaussian03. The CIS method actually predicts the vertically excited Franck–Condon state from which the charge transfer excited state arises. This method, using 6-31G+(d,p) as basis set, predicts that the cis form (having energy value $-875.326\,487\,59$ au) in the excited state is more stable than the trans form (having energy value $-874.769\,435\,82$ au). The excited-state dipole moment of the probe in water, ~ 2.20 D, is the same in both cis and trans states. The dipole moment change from the ground to the excited state in aprotic polar solvents is found to be 2.57 D, as measured from a Lipert–Mataga plot of experimental data. This result, with low dipole moment change along with near-planar structure in ground and excited states suggests that formation of the charge-transfer state does not depend on orthogonal rotation of the moieties.

A distinctive bathochromic shift caused by solvent polarity was noted for the second fluorescence band. The most interesting observation was in water; a drastically reversed trend of fluorescence spectra about 40 nm blue-shifted from DMSO. Usually the solvent dipoles reorient themselves around the fluorophore to attain an energetically favorable arrangement. In such an orientation, the dipole moment of the probe molecule is enhanced in the

excited state by stabilization of the CT state with increasing solvent polarity.²⁴ In the case of water, a highly polar protic solvent, the nature of the band is completely different. The blue shift may be due to stabilization of the ground state associated with a quinonoid to benzenoid transformation along with a new species that may be formed in water. To understand the phenomenon more clearly, the fluorescence emissions of DASQMI in different mixed solvents have been studied.

We used DMF–water binary solution to obviate the absence of any single solvent having a dielectric constant between those of DMSO and water. The basic idea of this experiment was to study the dual effect of dielectric constant and H-bonding ability. As we mixed water in DMF solution, initially a spectrum red-shifted 3 nm from DMSO was observed. On gradual addition of more water in DMF, a reversal of peak position was observed, and finally, with addition of even more water, this fluorescence peak position nearly matches with the peak position in neat water. It is important at this point to consider whether the H-bond donor ability of the solvent plays a role in stabilizing the low-energy charge-transfer state. Hydrogen-bond donor abilities of methanol, ethanol, and water are 0.83 , 0.93 , and 1.17 , respectively as determined by Kamlet et al.²⁵ Although the H-bond donor ability of DMSO is 0.0 , it stabilizes the charge-transfer state well. Ethanol, being closer to water with respect to H-bonding ability, does not cause any blue shift of emission in DASQMI. It appears, therefore, the hydrogen-bond donor ability of the solvent is not the only controlling factor for the stabilization of the excited state. So this experiment indicates that either the high polarity (dielectric constant) or a combined effect of both polarity and H-bonding ability of the solvent may play a crucial role in stabilizing the ICT state of the hydrophobic molecule in water.

To clarify this nature, we observed the fluorescence spectra (Figure 1) of DASQMI in D_2O solvent. In D_2O solvent, the hydrogen-bonding effect is absent but the dielectric constant is the same as that of water. Surprisingly, in D_2O solvent DASQMI shows the usual red shift of the long-wavelength band. So one would think that dielectric constant is not the only factor responsible for the blue shift of the fluorescence spectra in water. It is now clear that the dielectric constant or hydrogen-bonding effect (like ethanol) alone is not the deciding factor for the reverse nature of spectral shift in water. It may so happen that after reaching a certain dielectric constant, along with the protic character of the solvent, the ground state of the probe gets more stabilized than the excited state due to a benzenoid to quinonoid transformation. To understand the phenomenon more clearly, the emission of DASQMI in D_2O –ethanol mixed solvents has also been studied.

In general, for any binary mixture the fluorescence peak position always remains between the fluorescence peak positions of the molecule in those two pure solvents. DASQMI shows the emission peaks at 529 and 522 nm in pure D_2O solvent and in pure ethanol, respectively. But successive addition of ethanol in D_2O shifts the peak beyond the position 522 nm (point B in Figure 3, 20% ethanol, dielectric constant ~ 75) to 490 nm (point C in Figure 3, 40% ethanol), the maximum blue-shifted position, which is near the position in water (480 nm). Upon further addition of ethanol in D_2O , the peak starts moving toward red until 90% ethanol (520 nm, point D in Figure 3) is added. D_2O has a high dielectric constant with no hydrogen-bonding ability; on the other hand, ethanol has the hydrogen-bonding effect but the dielectric constant is low. In the region A–C in Figure 4, the progressive blue shift is due to the protic

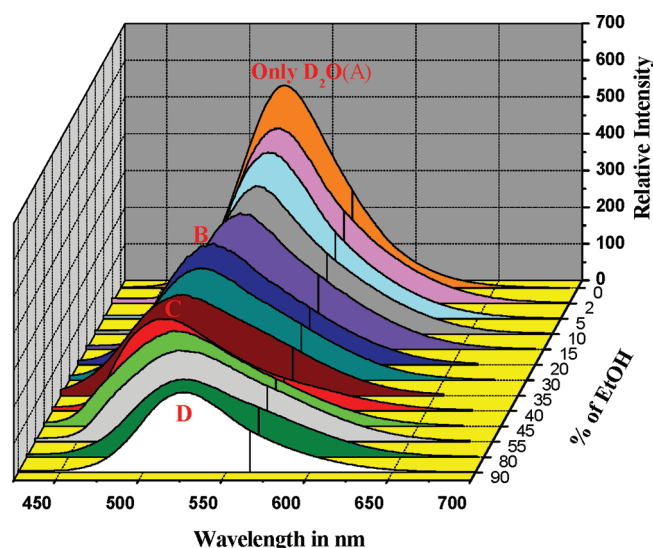


Figure 3. Spectral shift of DASQMI in binary mixture of D_2O and ethanol. (A) Neat D_2O , (B) like ethanol at room temperature, (C) critical point, 40% ethanol, from this point red shift starts, and (D) 90% ethanol.

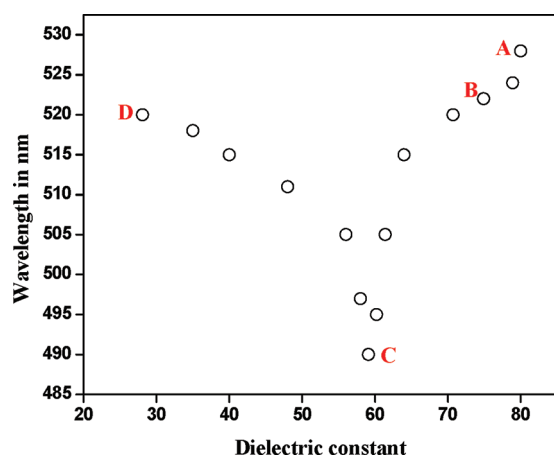


Figure 4. Variation of dielectric constant with unusual fluorescence peak shift of DASQMI in the presence of different percentages of ethanol in D_2O solution.

character of the mixture with sufficient value of dielectric constant, but beyond point C (dielectric constant ~ 60), the dielectric constant of the mixture goes below the critical value and a red shift starts up to point D (90% ethanol, dielectric constant ~ 27), like any protic solvent other than water. This experiment along with the earlier observations compel us to consider that, beyond a certain critical amount of dielectric constant (~ 60) of the solvent in the presence of protic character, the fluorescence peak position of DASQMI moves to higher energy, a case of “negative solvatochromism” as observed in merocyanine dyes.^{26–28} In all solvents the ICT state is stabilized with increasing solvent polarity and moves toward the ground state, and after a critical polarity and H-bonding ability, further stabilization of ground state yields a blue shift.

The steady-state emission anisotropy as a function of wavelength was measured in different solvents to determine the rotational motion about the flexible bonds. DASQMI shows a very

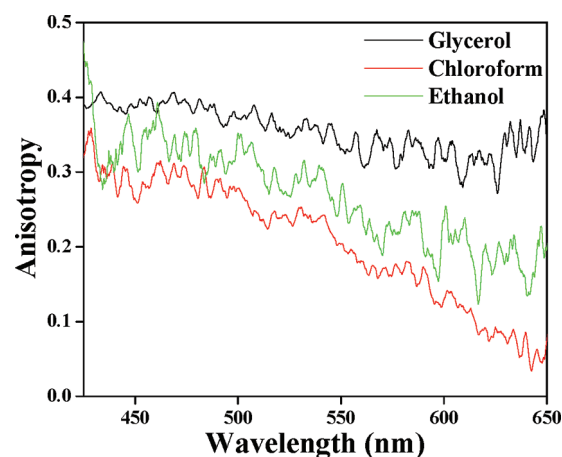


Figure 5. Steady-state emission anisotropy of DASQMI as a function of wavelength in glycerol, chloroform, and ethanol.

high value of steady-state anisotropy (0.38) in the initial part of the emission spectrum in all the solvents measured, which indicates that the transition dipole moment, that is, the molecular configuration during the emission from initially excited state, does not change. In glycerol, a nearly flat (from 0.38 to 0.35) anisotropy plot with increasing wavelength was observed, but in chloroform a considerable decrease (from 0.38 to 0.20) of anisotropy could be found with increasing wavelength (Figure 5). The gradual change in molecular configuration, and as a result decrease in anisotropy in nonviscous solvent, clearly indicates the character of the charge-transfer process to be ICT.

3.2. Low-Temperature Fluorescence. From the observations so far, we may propose that the formation of excited electronic state is accompanied by an internal conversion into a new state that has a much larger dipole moment. Solvent reorganization around the excited probe stabilizes the intramolecular charge-transfer state.²⁹ The solvent-stabilized charge-transfer state may cross over into the normal excited state at room temperature by solvent fluctuation, but as the temperature is lowered, such fluctuations diminish and as a result the polarity of the solvent increases at that environment.³⁰ This phenomenon may precisely explain the anomalous blue shift of the fluorescence peak position of the molecule in water. The fluorescence spectra of DASQMI in ethanol and methyl cyclohexane at 77 K have been recorded. In MCH the peak position was red-shifted along with a large increment of intensity compared to the room-temperature fluorescence. At low temperature the probe is subjected to a more rigid environment, causing a hindrance in rotation about the flexible single bond and other nonradiative processes, which helps to increase the CT emission.

In the case of ethanol glass matrix, a large increment of intensity was also observed, but the interesting thing is that the band shifts toward blue at 77 K, compared to the room-temperature fluorescence emission. At room temperature the H-bond parameter is nearly the same as that of water, but the dielectric constant is very low compared to that of water. The cause of fluorescence peak position reversal (blue) at 77 K might be due to more organized solvent molecules at that temperature, which pushes the dielectric constant to a higher value. So at low temperature, having H-bond ability and a large dielectric constant helps ethanol to stabilize the ground state more compared to the ICT state of the probe DASQMI in that environment.

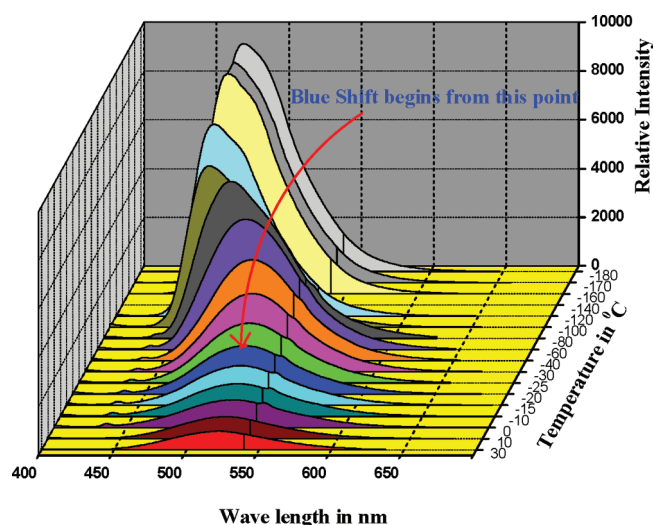


Figure 6. Spectral signature of DASQMI at 77 K and with the temperature increasing to room temperature.

To be sure that a trigger dielectric constant along with hydrogen-bonding effect is necessary for this unusual fluorescence spectral shift; fluorescence emission data in a wide temperature range (>77 K) have also been recorded (Figure 6). As the temperature is lowered from room temperature, the ethanol peak shifts toward red until the temperature reaches 253 K, and after that the emission peak starts moving toward blue, indicating the beginning of orientation of fluctuating solvent dipoles. The blue shift reaches a maximum at 193 K, showing the solvent dipoles orientation also to be maximum, and after that the same shift is maintained up to 77 K. This is somewhat similar to the emission in mixed D_2O –ethanol solvent (vide supra). But in MCH only regular red-shifted spectra were observed throughout. So it is now clear that after achieving a critical dielectric constant at <253 K, along with the protic character of the solvent, the ground state is stabilized more than the ICT state, and consequently the blue-shifted emission of the probe in that solvent could be observed. At 193 K ethanol attains the maximum dielectric constant, similar to water.

3.3. Time-Resolved Emission. Picosecond time-resolved fluorescence measurements were done for the probe in different solvents to characterize the spectral properties and dynamics, considering the polarity and H-bond effect on the excited state by the 390-nm photoexcitation. We have measured the lifetime of the species formed in the excited state by monitoring the emission at its corresponding steady-state emission wavelengths. After fitting the decay curve of the probe in different solvents, the fluorescence lifetime components we got are delineated in Table 2. Upon photoexcitation, the internal charge transfer from the electron-donating dimethylamino moiety to the electron-accepting quinolinium moiety results in the excited charge-transfer state. The new electronic charge distribution sets the relaxation of solvation energy by the reorganization of solvent molecules. The lifetime of DASQMI, regardless of collecting the emission at normal excited state or at charge-transfer bands, are found to fit well with a biexponential function as

$$I(t) = \sum_i D_i \exp(-t/\tau_i) \quad (2)$$

where τ_i , the fluorescence lifetime, is associated with the excited-state species and D_i is the pre-exponential factor. Analysis of the

Table 2. Fluorescence Lifetime of the Probe Molecule in Different Solvents^a

solvent	λ_{mon} (nm)	lifetimes						
		τ_1 (ns)	a_1	τ_2 (ns)	a_2	τ_3 (ns)	a_3	χ^2
MCH	430	1.44	0.80	2.68	0.20			0.98
EtOH	522	1.38	0.25	3.00	0.75			0.97
ACN	524	1.25	0.23	3.07	0.77			0.99
Gly	527	1.23	0.30	3.02	0.70			1.01
DMF	524	1.22	0.22	3.00	0.78			0.96
DMSO	528	1.20	0.18	3.40	0.88			0.99
D_2O	529	1.20	0.20	3.40	0.80			1.00
water	480	1.34	0.20	3.01	0.05	9.40	0.75	0.98

^a The samples were monitored at their charge-transfer band maxima ($\lambda_{\text{mon}} = 430$ –529 nm) in these solvents. Here τ_i and a_i are the lifetime and relative amplitude of the pre-exponential factors, respectively ($\lambda_{\text{exc}} = 295$ nm). χ^2 is the measure of good fitting and its range is 0.8–1.2.

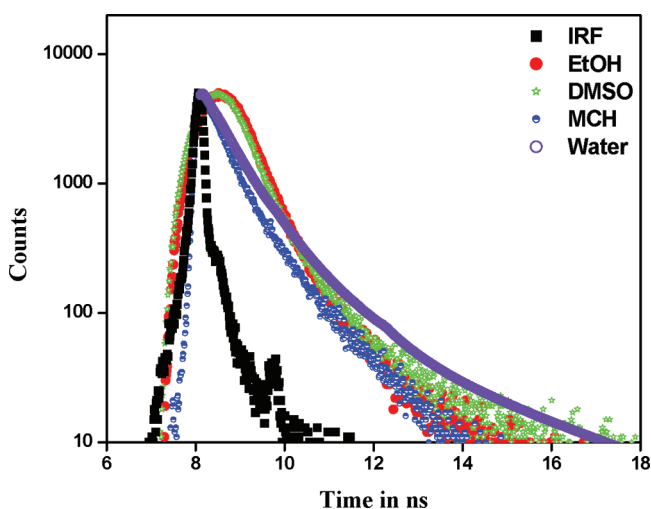
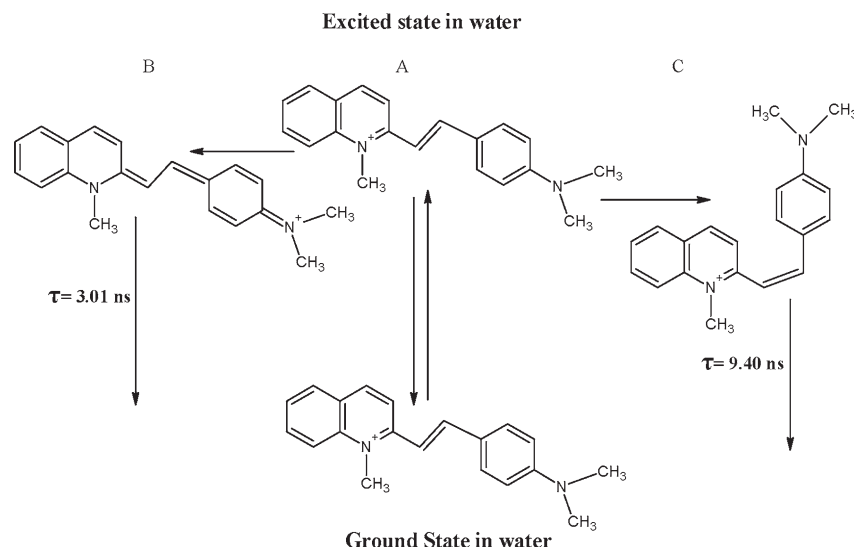


Figure 7. Time-resolved decay profile of the probe molecule in methylcyclohexene, DMSO, and water at room temperature, monitored at their corresponding steady-state emission wavelengths. (IRF = instrument response function.)

decay profile indicates the formation of two distinct species in all the solvents. In MCH, one species has a lifetime of 1.44 ns (relative abundance 80%) and the other is 2.68 ns (relative abundance 20%), and in ethanol, the values are 1.38 ns (25%) and 3.06 ns (75%). The gradual increase in amplitude of second band decay in solvents starting from MCH to DMSO (Figure 7) reflects the efficient conversion of second state from the first. But in water, along with the above-mentioned two components of fluorescence lifetime, we also find a third long-decay component having 75% relative abundance. The above observations point out that the fluorescence lifetime of the charge-transfer state increases as we go from lower dielectric constant to the higher dielectric constant of the medium, and as the dielectric constant increases above a critical value, with H-bonding ability, the new component arises. The larger fluorescence lifetime for the second component in DMSO (3.4 ns) and D_2O (3.4 ns) is due to the absence of H-bond in the solvent as well as the hydrogen-bonding-related nonradiative path. In the case of a viscous solvent, glycerol, the second component (charge transfer) is nearly

Scheme 1



equal to ACN, which confirms that charge-transfer band does not arise due to the rotation of single bond of the molecule. So the long-wavelength band may safely be designated as due to intramolecular charge transfer. For the solvents other than water, a possible explanation for the increase in τ_f may be due to the rearrangement of electronic excited states with increasing solvent polarity. In water, which has a large dielectric constant and H-bonding character, a new decay component arises. So it is clear that the dielectric constant and the H-bond effect (above a critical dielectric constant) of the local environment affect the excited species formation strongly. Looking at anomalous emission in water and also at time-resolved data in water, we may propose that, upon photoexcitation after some critical point, the ICT state becomes the ground state so that its further stabilization with solvents results in a blue shift (thus causing negative solvatochromatism), and a possibly cis form (Scheme 1) having a slow component in fluorescence lifetime could be observed, which is not observed in other solvents as well as in “water-like situations”. The same indication has already been predicted from theoretical calculations. In D_2O , which has the same dielectric constant as water, we observe two decay components like other solvents. As we add EtOH in D_2O gradually, we find the third long-lifetime component appearing, the amplitude of which increases with EtOH concentration, and in pure water the long-lifetime component dominates with amplitude of $\sim 75\%$.

4. CONCLUSION

From the experimental observations and also from the quantum chemical calculations, it is clear that the nature of excited-state charge transfer is intramolecular type (ICT) and not twisted intramolecular charge transfer, as energy does not get minimized in the excited state due to geometry deformation. The steady-state fluorescence as a whole indicates that the excited intramolecular charge-transfer state is stabilized progressively in solvents of rising dielectric constant and H-bonding ability, but after some critical point the ICT state becomes the ground state so that its further stabilization with solvents results in a blue shift (thus causing negative solvatochromism). This phenomenon is observed in water as well as in “water-like situations”. Presence of an

additional slow component in the fluorescence lifetime decay with nearly 75% amplitude in water necessitates us to conceive a possible formation of cis-isomer due to the highly hydrophobic nature of the probe in addition to ground-state stabilization and associated blue shift.

AUTHOR INFORMATION

Corresponding Author

*E-mail spsc@iacs.res.in.

ACKNOWLEDGMENT

We gratefully acknowledge Dr. Abhijit Kumar Das, Mr. Debasish Mandal, and the Aneesur Rahman High Performance Computing Centre, IACS, for helping in theoretical calculations. We thank the reviewers for their helpful suggestions to improve the paper, and we also express thanks to Mr. Subrata Das, Department of Spectroscopy, IACS, for taking picosecond time-resolved data.

REFERENCES

- (1) Lippert, E.; Lüder, W.; Moll, F.; Nägele, W.; Boos, H.; Prigge, H.; Seibold-Blankenstein, I. *Angew. Chem.* **1961**, *73*, 695–706.
- (2) Lippert, E.; Rettig, W.; Bonacic-Koutecký, V.; Heisel, F.; Miehé, J. A. *Adv. Chem. Phys.* **1987**, *68*, 1–173.
- (3) Zachariasse, K. A.; von der Haar, T.; Hebecker, A.; Leinhos, U.; Kühnle, W. *Pure Appl. Chem.* **1993**, *65*, 1745–1750.
- (4) von der Haar, T.; Hebecker, A.; Il'ichev, Y.; Jiang, Y. B.; Kühnle, W.; Zachariasse, K. A. *Recl. Trav. Chim. Pays-Bas* **1995**, *114*, 430–442.
- (5) Sobolewski, A. L.; Domcke, W. *Chem. Phys. Lett.* **1996**, *250*, 428–436.
- (6) Sobolewski, A. L.; Domcke, W. *Chem. Phys. Lett.* **1996**, *259*, 119–127.
- (7) Grabowski, Z. R.; Rotkiewicz, K.; Siemiarz, A.; Cowley, D. J.; Baumann, W. *Nouv. J. Chim.* **1979**, *3*, 443–454.
- (8) Rotkiewicz, K.; Grellmann, K. H.; Grabowski, Z. R. *Chem. Phys. Lett.* **1976**, *19*, 315–318.
- (9) Bangal, P. R.; Chakravorti, S.; Mustafa, G. J. *Photochem. Photobiol.* **1998**, *113*, 35–43.

- (10) Saroja, G.; Soujanya, T.; Ramachandram, B.; Samanta, A. *J. Fluoresc.* **2008**, *8*, 405–410.
- (11) Gao, L.; Song, Q.; Huang, X.; Huang, J. *J. Colloid Interface Sci.* **2008**, *323*, 420–425.
- (12) Herbich, J.; Karpiuk, J.; Grabowski, Z. R.; Tamai, N.; Yoshihara, K. *J. Lumin.* **1992**, *54*, 165–175.
- (13) Rotkiewicz, K.; Rettig, W. *J. Lumin.* **1992**, *54*, 221–229.
- (14) Shin, D. M.; Whitten, D. G. *J. Phys. Chem.* **1988**, *92*, 2945–2958.
- (15) Bangal, P. R.; Panja, S.; Chakravorti, S. *J. Photochem. Photobiol. A* **2001**, *139*, 5–16.
- (16) Strehmel, B.; Rettig, W. *J. Biomed. Opt.* **1996**, *1*, 98–109.
- (17) Ramadass, R.; Hahn, J. B. *J. Phys. Chem. B* **2007**, *111*, 7681–7690.
- (18) Loew, L. M.; Bonneville, G. W.; Surow, J. *Biochemistry* **1978**, *17*, 4065–4071.
- (19) Loew, L. M.; Scully, S.; Simpson, L.; Waggoner, A. S. *Nature* **1979**, *281*, 497–499.
- (20) Chowdhury, P.; Panja, S.; Chakravorti, S. *J. Phys. Chem. A* **2003**, *107*, 83–90.
- (21) Mitra, S.; Tamai, N. *Chem. Phys.* **1999**, *246*, 463–475.
- (22) O'Connor, D. V.; Phillips, D. *Time-correlated single photon counting*; Academic Press: New York, 1984; Chapt. 6.
- (23) Frisch, J. M.; Pople, J. A. et al. Gaussian 03, revision C.03; Gaussian, Inc., Wallingford, CT, 2004.
- (24) Dekhtyar, M.; Rettig, W.; Weigel, W. *Chem. Phys.* **2008**, *344*, 237–250.
- (25) Kamlet, M. J.; Abboud, J. L. M.; Abraham, M. H.; Taft, R. W. *J. Org. Chem.* **1983**, *48*, 2877–2887.
- (26) Botrel, A.; Le Beuze, A.; Jacques, P.; Strub, H. *J. Chem. Soc., Faraday Trans. 2* **1984**, *80*, 1235–1252.
- (27) Jacques, P. *J. Phys. Chem.* **1986**, *90*, 5535–5539.
- (28) Botrel, A.; Aboab, B.; Corre, F.; Tonnard, F. *Chem. Phys.* **1995**, *194*, 101–116.
- (29) Verhoeven, J. W. *Top. Fluoresc. Spectrosc.* **2005**, *9*, 249–284.
- (30) Bulitz, G. U.; Boxer, S. G. *J. Am. Chem. Soc.* **1998**, *120*, 3988–3992.